Radiocarbon (2026), **68**, pp. 1062–1070
doi:10.1017/RDC.2025.10149

Selected Papers from the 4th Radiocarbon in the Environment Conference, Lecce, Italy, 23–27 Sept. 2024

CONFERENCE PAPER

Radiocarbon dating of a monumental dragon tree (*Dracaena draco* (L.) L.)

Franco Biondi[1], Guaciara M. Santos[2], Jordan Palli[3], Gianluca Piovesan[3] and Pedro A. Sosa[4]

[1]DendroLab, Dept. of Natural Resources and Environmental Science, University of Nevada, Mail Stop 0186, Reno, NV 89557-0186, USA, [2]Department of Earth System Science, University of California Irvine, Irvine, CA 92697-3100, USA, [3]Department of Ecological and Biological Sciences (DEB), University of Tuscia, Largo dell'Università snc, 01100 Viterbo, Italy and [4]Instituto Universitario de Estudios Ambientales y Recursos Naturales (IUNAT), Universidad de Las Palmas de Gran Canaria, Canary Islands, Spain
Corresponding author: Franco Biondi; Email: franco.biondi@dendrolab.org

Received: 20 January 2025; **Revised:** 25 April 2025; **Accepted:** 22 May 2025; **First published online:** 16 October 2025

Keywords: arboreal monocotyledons; ^{14}C AMS; Canary Islands; plant longevity; wiggle-matching

Abstract

Some arboreal monocotyledons, such as the dragon trees (*Dracaena* sp.), can develop impressive trunks (>5 m perimeter) through a lateral meristem, but their ages are difficult to determine. We report here a series of calibrated radiocarbon (^{14}C) dates obtained from a stem section of *Dracaena draco* (L.) L. subsp. *draco* growing on the island of Tenerife, Canary Islands, Spain. This radial section, about 40 cm long, was cut on October 18, 2023, from a large (~60 cm diameter) branch that had fallen off the main stem of a privately owned dragon tree. In order to apply ^{14}C calibration, and given the lack of clearly defined growth layers, we collected 33 sequential samples at ~1-cm intervals along this radial section. A first attempt at wiggle-matching resulted in a calibrated dating of ~1787 CE for the innermost sample. Because we only knew the spatial distance, but not the time interval, between ^{14}C dates, we further applied calibration tools commonly used for sedimentary sequences. The Poisson-process deposition model in the software OxCal resulted in a calibrated age for the innermost sample of 1776–1798 CE (2σ). The classic and Bayesian age-depth deposition models available as R packages dated the innermost sample to, respectively, 1775–1862 and 1768–1813 CE. Because the branch was at a height of ~3 m from the ground, and its section did not reach the pith, our results suggest that this dragon tree was ~300 years old in 2023.

Introduction

Dragon trees, i.e. arboreal *Dracaena* spp., are ancient monocotyledons still found naturally in tropical and subtropical habitats surrounding the Sahara Desert (Maděra et al. 2021). Among them, *Dracaena draco* (L.) L. subsp. *draco* is a species endemic to the Macaronesian region (i.e., the archipelagos of Madeira, Canary Islands, and Cape Verde) and the Moroccan Anti-Atlas. The largest dragon trees, which can reach ~20 m in height and in circumference, are iconic plants characterized by large roots, which sometimes merge with the thick, erect trunk at the base. Their growth, after an initial height increase, is characterized by sympodial branching, i.e., each branch order is created from a sleeping lateral bud growing up after an apical leaf rosette blooms and the terminal bud dies. This process usually takes place after the flowering process, so that older individuals have a highly divided, fan-shaped crown (Lengálová et al. 2020). In addition, peripheral branches, which have a characteristic "sausage-shaped" form, have been used to infer plant age together with the number of growth tops either flowering or not (Adolt et al. 2012; Adolt and Pavlis 2004).

© The Author(s), 2025. Published by Cambridge University Press on behalf of University of Arizona. This is an Open Access article, distributed under the terms of the Creative Commons Attribution licence (https://creativecommons.org/licenses/by/4.0/), which permits unrestricted re-use, distribution and reproduction, provided the original article is properly cited.

Downloaded from https://www.cambridge.org/core. IP address: 217.74.153.144, on 01 Oct 2026 at 02:10:25, subject to the Cambridge Core terms of use, available at https://www.cambridge.org/core/terms. https://doi.org/10.1017/RDC.2025.10149

Besides their botanical and conservation value, dragon trees have acquired numerous social and cultural meanings, including traditional and medicinal significance related, for example, to the valuable crimson red resin known as "dragon's blood" (Gupta et al. 2008). A famous dragon tree, located at Icod de los Vinos in Tenerife, reaches a height of ∼18 m and a basal stem circumference of ∼18.5 m; it is thought to be several centuries old according to the most recent estimates (Lengálová et al. 2020). Many aspects of the species' physiology and reproductive biology are unknown (Durán et al. 2020), and it is unclear why in the Canary Islands dragon trees are found naturally only on the islands of Tenerife and Gran Canaria, while they are absent in their natural state on other islands such as La Gomera and La Palma. The 694 wild specimens found on Tenerife are located almost entirely in the older geological areas of the island: the massifs of Anaga, Teno and Adeje, with a total area of 21.8 km^2 (Almeida Pérez 2004).

The species is considered "Endangered (EN B2ab(ii,iii,iv,v)) as a result of the restricted area of occupancy, severe fragmentation, and the ongoing decline in the quality and area of habitat" (Silva et al. 2021). As a consequence, in recent years there has been renewed research efforts aimed at understanding its germination responses (Cartereau et al. 2023), root and stem growth anatomy (Jura-Morawiec et al. 2021; Marcinkiewicz and Jura-Morawiec 2024), aerial roots function (Krawczyszyn and Krawczyszyn 2014), and maximum lifespan (Biondi et al. 2024). This latest aspect is closely linked with the analysis of plant life history and growth patterns, but age estimation models based on identifying past growth patterns from current external features are not entirely satisfactory, and a review of the scientific literature on dragon trees concluded that "we still do not understand how to estimate age reliably" (Maděra et al. 2020).

A scientific ageing tool for plants with secondary growth that do not form clear rings is radiocarbon (^{14}C) dating, which is gaining increasing popularity because of technological advances and widespread applications (Palli et al. submitted). Since the late 1970s, accelerator mass spectrometry (AMS) has made ^{14}C dating more affordable by reducing sample sizes (∼100 times smaller than those needed for decay counting) and providing faster results (days rather than weeks). Breakthroughs over the last two decades have led to further reduction of mass requirements (Santos et al. 2007) as well as higher reliability of the produced results (Bronk Ramsey 2023), thus reducing ^{14}C age uncertainties. But since radiocarbon values are affected by fluctuations in ^{14}C production rates caused by solar activity or changes in the Earth's magnetic field, calibration of radiocarbon ages is still needed.

The massive input of excess-^{14}C due to nuclear bomb tests between 1955 and 1963 allows us to resolve calendar ages within 1–2 years. The post-1950 CE period is therefore commonly referred to as "post-bomb" while prior years become "pre-bomb". Recent ^{14}C dataset revisions and new additions have allowed to refine the post-bomb global compilations and extended them to 2019 (Hua et al. 2022). Therefore, the IntCal post-1950 datasets have helped with determining annual growth patterns of pantropical tree species with poorly defined anatomical features (i.e., vague, discontinuous, false, and absent tree rings). With this approach, lack of seasonality has been found in *Juniperus procera* from Ethiopia (Wils et al. 2009), *Hymenaea courbaril* from southwestern Brazilian Amazonia (Santos et al. 2021), *Araucariaceae* and *Callitris* species of Australia (respectively, Haines et al. 2018; Pearson et al. 2011). Complex growth trends, such as biannual formation in *Cedrela odorata* from Suriname, have also been evaluated using post-1950 ^{14}C analysis (Baker et al. 2017), and ^{14}C dating has overall favored the selection of woody species suitable for tropical tree-ring studies (Giraldo et al. 2023; Groenendijk et al. 2014; Santos et al. 2024; Soliz-Gamboa et al. 2011).

Pre-bomb calibration curves to convert ^{14}C dates to calendar years are also available to users (Reimer et al. 2020). During pre-bomb periods, dating accuracy has been improved by matching radiocarbon dates to the 'wiggles' of the calibration curve when the age difference between the ^{14}C dates is known (Bronk Ramsey et al. 2001). However, when only the spatial distance between sequential radiocarbon samples is available, but not the exact time interval, a different approach needs to be used. In this case, "deposition models" (Bronk Ramsey 2008) have been developed for radiocarbon calibration of sedimentary sequences and other chronologically ordered sample sequences (Hua et al. 2012; Piotrowska et al. 2010). Building from previous investigations (Biondi et al. 2024), and because of the

Downloaded from https://www.cambridge.org/core. IP address: 217.74.153.144, on 01 Oct 2026 at 02:10:25, subject to the Cambridge Core terms of use, available at https://www.cambridge.org/core/terms. https://doi.org/10.1017/RDC.2025.10149

Figure 1. *Photograph of the radial section that was cut from the dragon tree branch (see Figure S4 in Biondi et al. 2024). A total of 33 samples were collected at ~1 cm from each other (see ruler at the bottom for scale) and numbered progressively from the innermost to the outermost portion of the section. The last sample (# 33) was approximately 4 cm from the bark.*

need to clarify the maximum lifespan of dragon trees, we report here on a new set of AMS radiocarbon dates that were calibrated using wiggle-matching and three different models, namely the Poisson-process deposition model in OxCal (Bronk Ramsey 2008), the linear regression age-depth model (Blaauw 2010) and the Bayesian age-depth model (Blaauw and Christen 2011).

Methods

Sample collection

The sampled dragon tree, which was already described by Biondi et al. (2024), is located in Tenerife, Canary Islands, Spain (Figure S1). Its estimated age, according to local land managers, is ~330 years; single-sample ^{14}C-AMS dating had suggested an age of ~350 years for this dragon tree, but with large errors and other, more recent, potential calibration matches. A large (~60 cm diameter) branch had fallen to the ground and a cross-section was cut in the owner's backyard on October 18, 2023. After cutting the branch cross-section, a smaller piece was cut in the radial direction, from the outside all the way to the inner circular cavity located inside the stem (Figure S4 in Biondi et al. 2024). The radial section, about 40 cm long, was then transported to the DendroLab, where it was left to dry. The wood was very moist, as shown by fungi growing inside the stem cavity; the same fungi later developed on the smaller piece when it was left out to dry (Figure S4c in Biondi et al. 2024).

At the DendroLab, the branch section was surfaced and polished using progressively finer sandpaper, first with a belt sander, then with an orbital sander, and finally by hand, all the way to >600 grits. Wood samples from the branch section were then manually collected using a steel chisel and at regular intervals, about 1 cm from each other, starting from the innermost portion and proceeding towards the outer, more recent growth tissues (Figure 1). Each sample was weighted to make sure it exceeded 30 mg (Table S1) to allow for successful chemical and isotopic analyses.

Radiocarbon dating

The ^{14}C analyses were performed at the Keck Carbon Cycle Accelerator Mass Spectrometry (KCCAMS) Laboratory at the University of California, Irvine (USA). Samples were reduced to particles (~0.06 × 1 cm) and then individually processed to cellulose following previously published methods (Santos et al. 2023). To summarize, samples were extracted to holocellulose by cycling HCl and NaOH at 70°C for 30 min and then bleached with a 1:1 NaClO/1N HCl at 70°C for

Downloaded from https://www.cambridge.org/core. IP address: 217.74.153.144, on 01 Oct 2026 at 02:10:25, subject to the Cambridge Core terms of use, available at https://www.cambridge.org/core/terms. https://doi.org/10.1017/RDC.2025.10149

4 hr. Afterwards, samples were rinsed with 1N HCl @70°C for 10 min, and brought to pH 6–7 with warm MilliQ water. Once the samples were combusted alongside of reference materials (i.e., samples of known age and blanks), fast and complete graphitization was performed by the Zn-method (Santos and Xu 2017; Xu et al. 2007) followed by isotopic analysis. Even though efficiency of holocellulose extraction led to relatively low yields (Table S1), filamentous graphite targets produced in this study were ≥ 0.6 mg C.

^{14}C-AMS measurement was performed on an in-house modified National Electrostatics Corporation (NEC 0.5MV 1.5SDH-21 model) spectrometer. This instrument is equipped with ^{13}C and ^{12}C measurements, allowing for online isotopic-fractionation corrections, and consequently produces high-precision ^{14}C results (Beverly et al. 2010). A total of 7 Oxalic Acid I (OX-I or NIST HOxI SRM 4990B) as combustible graphite targets were used as the primary standard, followed by Oxalic acid II (OXII, NIST SRM 4990C) as secondary. For chemical blank and secondary standards, we made use of the AVR ancient wood, FIRI-H sub-fossil wood and FIRI-J modern barley. Radiocarbon results were analyzed following procedures described in Santos et al. (2007) and later were expressed as fraction modern carbon (F^{14}C) and/or ^{14}C age BP followed by uncertainties (Stuiver and Polach 1977) before calibration to calendar years took place. The individual statistical error bars of the ^{14}C data were calculated based on counting statistics and propagated uncertainties due to normalization and processing of blanks. Reproducibility was better than 0.3% using reference materials (as combustibles and/or holocellulose). Samples labeled "Modern" contained an excess of ^{14}C from mid-20th century atmospheric thermonuclear weapons tests.

A simplified wiggle-match model of the pre-bomb radiocarbon ages (Barclay et al. 2023, 2024) against the IntCal20 curve (Reimer et al. 2020) was initially used. Since we had no information on time intervals between the sequential samples, we further analyzed the ^{14}C data by means of deposition models. First, we applied the Poisson-process model in the OxCal software, which allows for fluctuations in the deposition rate according to the depth of samples along the sequence (Bronk Ramsey 2009a; b). Then, we implemented two similar approaches commonly used for age-depth modeling of sedimentary records to reconstruct deposition histories. One was the linear regression model in the R package "clam" (Blaauw et al. 2025) and the other was the Bayesian model of the R package "rbacon" (Blaauw et al. 2024). Age-depth (deposition) models were run with all 33 samples; pre-bomb dates were calibrated using the IntCal20 curve (Reimer et al. 2020) while post-bomb dates were calibrated using the NH zone 2 curve (Hua et al. 2022) in the CALIBomb program (Reimer and Reimer 2025; Reimer et al. 2004). Applying deposition models to plant growth samples provided a narrower probability distribution for dating the innermost sample, and also an estimation of growth rate changes.

Results and discussion

As previously reported for arboreal palms (Tomlinson 2006), dragon trees can store large amounts of moisture inside their stem. Based on the moist and dry weight of our branch radial section, water content was ~50%. Macroscopically the surfaced and polished branch section seemed to show increment growth layers. When enlarged, the apparent banding was caused by varying orientation of the vascular bundles rather than cellular anatomy (Figure 2). These amphivisal secondary vascular bundles, where the xylem surrounds the phloem, are embedded in secondary, parenchymatous ground tissue, forming a peculiar type of ''wood'' (Jura-Morawiec 2015; Tomlinson and Zimmermann 1969).

Of the ^{14}C-AMS-dated samples, the last 11 (23–33) were initially categorized as "modern" (Table S1), i.e. post-1950, following the bomb-spike pattern in ^{14}C concentrations that has been recognized worldwide (Hua et al. 2022). The Poisson-process deposition model in OxCal indicated consistency of ^{14}C dates and identified a reduced probability distribution for 18 pre-bomb dates included in the model (Figure 3). The innermost sample resulted in a calibrated age (2σ) between 1776 and 1798 CE. This

Downloaded from https://www.cambridge.org/core. IP address: 217.74.153.144, on 01 Oct 2026 at 02:10:25, subject to the Cambridge Core terms of use, available at https://www.cambridge.org/core/terms. https://doi.org/10.1017/RDC.2025.10149

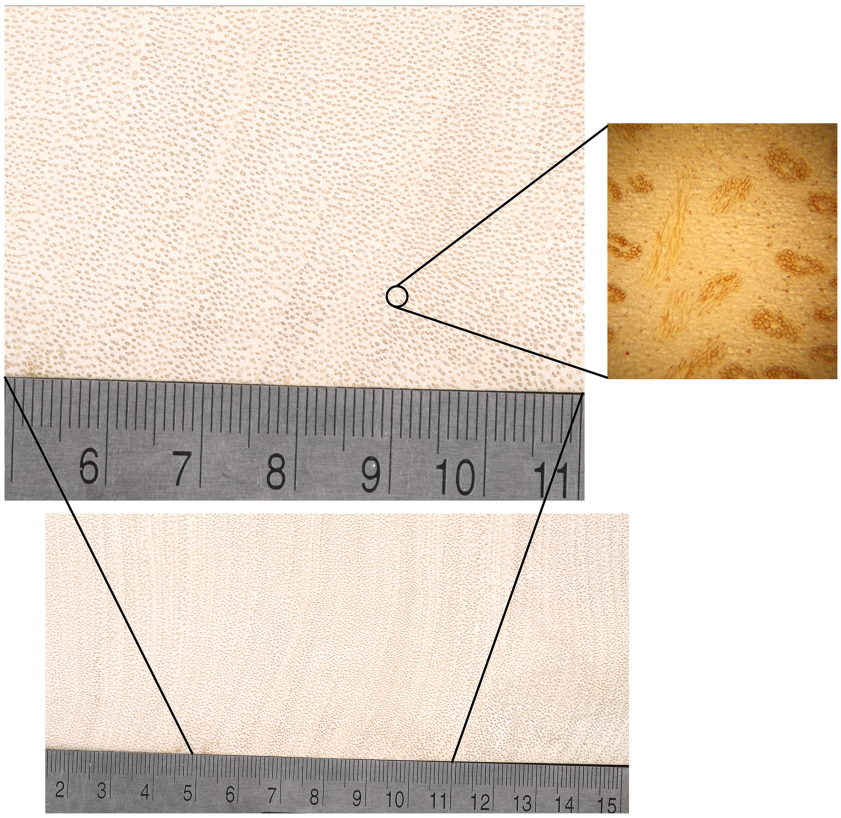

Figure 2. *Progressively enlarged photographs of the dragon tree section, surfaced and polished enough to show a macroscopic structure that vaguely resembles growth layers, but in reality is composed of a relatively uniform parenchyma matrix in which the amphivisal vascular bundles are embedded (Tomlinson and Zimmermann 1969).*

result is consistent with the simplified method of Barclay et al. (2023), which provided an estimated innermost sample year of 1787 CE (Figure S2).

Based on the CALIBomb results (Figure S2), sample 24 corresponds to ~year 1962 (next to the peak in ^{14}C) and sample 33 corresponds to ~year 1994. Since the outside of the branch shows signs of partial erosion and possibly insect galleries, it is difficult to estimate when it stopped growing. As we have about 9 cm between samples 24 and 33, covering a period of about 33 years, we can roughly estimate that the radial growth rate in the outer portion of this branch was approximately 3–4 yr cm^{-1}, while the preliminary wiggle-matching results suggested up to 6-12 yr cm^{-1} growth rates in the interior part. The linear regression model results produced by package "clam" suggest an average growth rate of 5.8 yr cm^{-1} (Figure 4). However, both the OxCal and the "rbacon" model indicate changes in growth rates occurred after ~1900 CE (Figure 4).

Considering that this branch section does not include its central part, we can estimate that the sampled branch was starting to form ~250 years ago. Given that such branch was already at a height of ~3 m from the ground, our new set of ^{14}C dating analyses suggests that this dragon tree was ~300 years old in 2023, thereby confirming and further refining the preliminary results obtained by Biondi et al. (2024). It should be mentioned that, thanks to a long sequence of ^{14}C dates, we reached this conclusion by applying to arboreal plants with secondary growth a set of radiocarbon calibration tools usually applied to sedimentary and depositional records. We therefore propose that using our approach can

Downloaded from https://www.cambridge.org/core. IP address: 217.74.153.144, on 01 Oct 2026 at 02:10:25, subject to the Cambridge Core terms of use, available at https://www.cambridge.org/core/terms. https://doi.org/10.1017/RDC.2025.10149

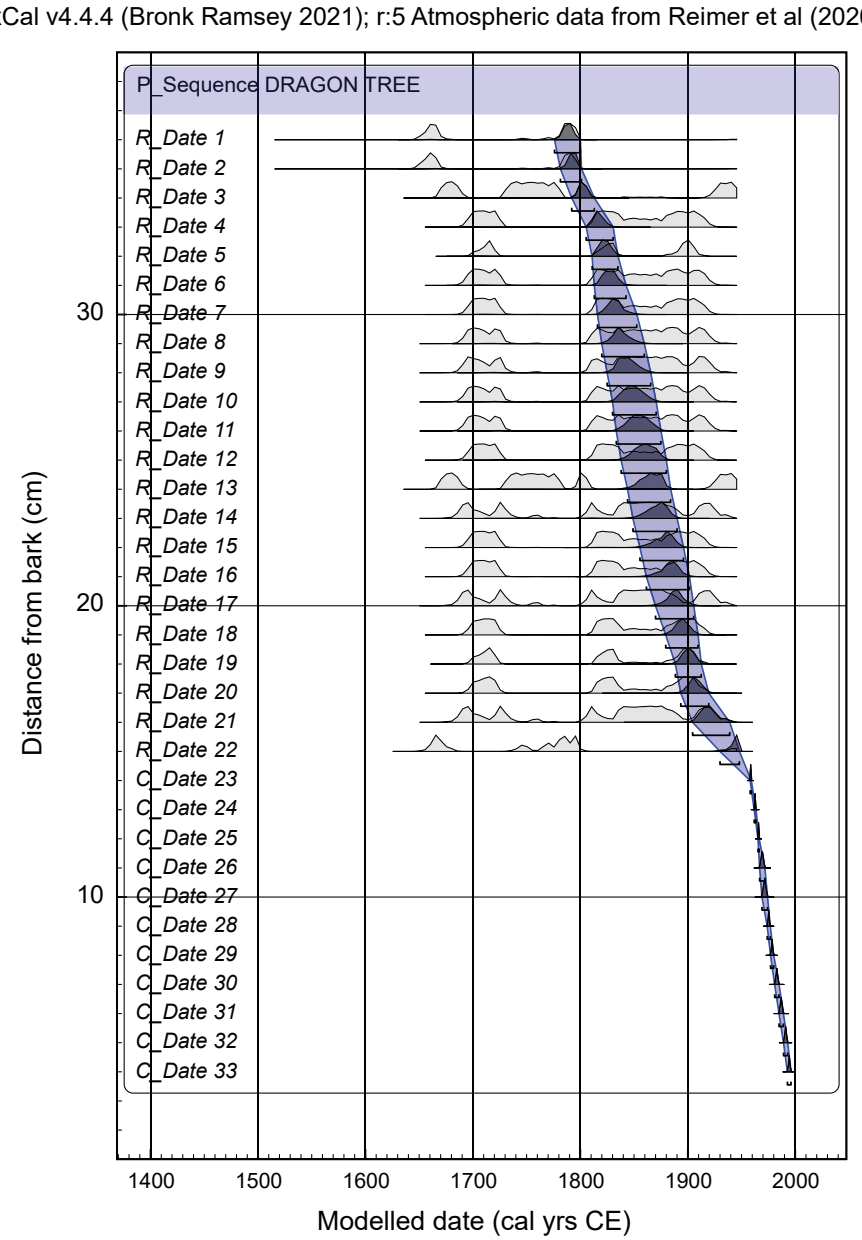

Figure 3. *Output from the Poisson-process deposition model in OxCal (Bronk Ramsey 2024) with* $A_{model} = 36.78$ *and* $A_{overall} = 30.73$*. Dates were assigned to a relative depth expressed as centimeters from the outer surface of the branch radial section and then calibrated using the IntCal20 curve (Reimer et al. 2020). Post-bomb dates were calibrated using the NH zone 2 curve (Hua et al. 2022) in the CALIBomb software, as shown in Figure S2, and then included in this model as calendar ages (C_dates).*

facilitate dating wood samples when no clear growth layers can be identified and/or the time interval between such layers is unknown.

Monumental plants of impressive size are examples of charismatic megaflora (Hall et al. 2011), whose presence usually becomes a synonym of sustainable land stewardship, prompting local

Downloaded from https://www.cambridge.org/core. IP address: 217.74.153.144, on 01 Oct 2026 at 02:10:25, subject to the Cambridge Core terms of use, available at https://www.cambridge.org/core/terms. https://doi.org/10.1017/RDC.2025.10149

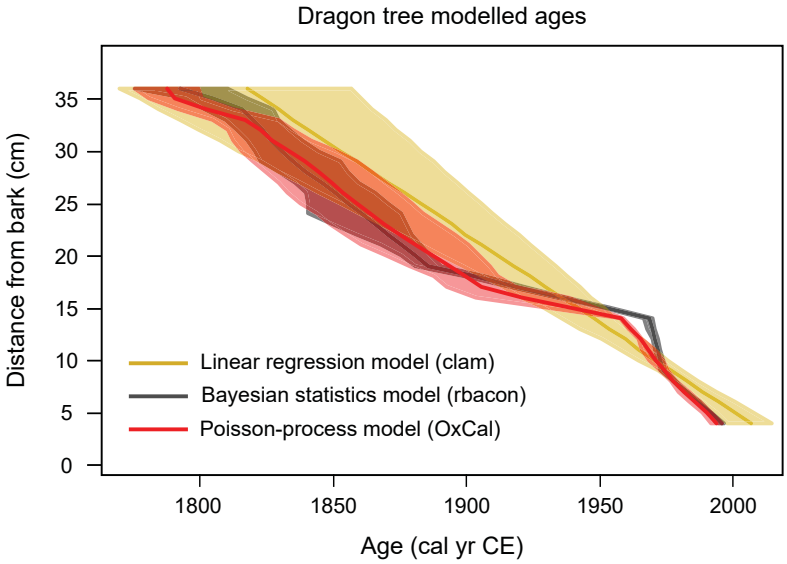

Figure 4. *Comparison between three different deposition models used for radiocarbon calibration. Pre-bomb dates were calibrated using the IntCal20 curve (Reimer et al. 2020); post-bomb dates were calibrated using the NH zone 2 curve (Hua et al. 2022).*

communities to advertise their location and old ages. Our contribution is aimed at applying the most advanced scientific dating tools to estimate the longevity of arboreal monocotyledons so that it is properly reported in both technical and lay-person documents.

Supplementary material. To view supplementary material for this article, please visit https://doi.org/10.1017/RDC.2025.10149

Acknowledgments. We are grateful to the local landowners and managers for allowing us to sample the monumental plant described in this article. In addition, we thank Francesco Salomone, José Alberto Delgado, Marcos Díaz Bertrana, Paulino Melchor, Nayra Méndez and Jesús Navarro for their help in collecting samples. Many thanks also to the Cabildo de Tenerife for their logistical support during field work. G.M.S. thanks the valuable help of the undergraduate students from the University of California-Irvine, Lucas Duy Nguyen and June Nakachi Griffin, on sample processing for ^{14}C-AMS dating. F.B. was funded in part by a Fulbright U.S. Senior Scholar award administered by the Commission for Cultural, Educational, and Scientific Exchange between the USA and Spain; the Experiment Station of the College of Agriculture, Biotechnology, and Natural Resources, the Ozmen Institute for Global Studies, the Office of the Provost, and the Faculty Research Travel Grant at the University of Nevada, Reno, USA.

Competing of interest. The authors declare no financial conflicts of interest.

References

Adolt R, Habrova H and Madera P (2012) Crown age estimation of a monocotyledonous tree species *Dracaena cinnabari* using logistic regression. *Trees - Structure and Function* **26**(4), 1287–1298. doi: 10.1007/s00468-012-0704-9.

Adolt R and Pavlis J (2004) Age structure and growth of *Dracaena cinnabari* populations on Socotra. *Trees - Structure and Function* **18**(1), 43–53. doi: 10.1007/s00468-003-0279-6.

Almeida Pérez RS (2004) *Dracaena draco* (L.) L. In Bañares A, Blanca G, Güemes J, Moreno JC and Ortiz S (eds), *Atlas y Libro Rojo de la Flora Vascular Amenazada de España*. Madrid, Spain: Publicaciones de O.A.P.N.

Baker JCA, Santos GM, Gloor M and Brienen RJW (2017) Does *Cedrela* always form annual rings? Testing ring periodicity across South America using radiocarbon dating. *Trees - Structure and Function* **31**(6), 1999–2009. doi: 10.1007/s00468-017-1604-9.

Barclay DJ, Haeussler PJ and Witter RC (2024) Dating the penultimate great earthquake in south-central Alaska using tree-ring crossdating and radiocarbon wiggle-matching. *Quaternary Science Advances* **13**, 100142. doi: 10.1016/j.qsa.2023.100142.

Barclay DJ, Witter RC and Haeussler PJ (2023) *WiggleMatch: A Spreadsheet for Radiocarbon Wiggle-Matching*. U.S. Geological *Survey*. doi: 10.5066/P943CGPB. Available at: https://code.usgs.gov/asc/wigglematch/-/tree/v1.0.0.

Downloaded from https://www.cambridge.org/core. IP address: 217.74.153.144, on 01 Oct 2026 at 02:10:25, subject to the Cambridge Core terms of use, available at https://www.cambridge.org/core/terms. https://doi.org/10.1017/RDC.2025.10149

Beverly RK, Beaumont W, Tauz D, Ormsby KM, von Reden KF, Santos GM and Southon JR (2010) The Keck Carbon Cycle AMS Laboratory, University of California, Irvine: Status Report. *Radiocarbon* **52**(2), 301–309. doi: 10.1017/S0033822200045343.

Biondi F, Santos GM, Rodríguez PR and Sosa PA (2024) Longevity estimates of Canary palms and dragon trees via radiocarbon dating: Initial results. *Plants* **13**(1), art. 45 (12 pp.). doi: 10.3390/plants13010045.

Blaauw M (2010) Methods and code for "classical" age-modelling of radiocarbon sequences. *Quaternary Geochronology* **5**(5), 512–518. doi: 10.1016/j.quageo.2010.01.002.

Blaauw M and Christen JA (2011) Flexible paleoclimate age-depth models using an autoregressive gamma process. *Bayesian Analysis* **6**(3), 457–474. doi: 10.1214/ba/1339616472.

Blaauw M, Christen JA, Aquino Lopez MA, Esquivel Vazquez J, Gonzalez OMV, Belding T, Theiler J, Gough B and Karney C (2024) Package "rbacon": Age-Depth Modelling Using Bayesian Statistics. Version 3.3.1. R Foundation for Statistical Computing. Available at: https://cran.r-project.org/web/packages/rbacon/index.html.

Blaauw M, Christen JA, Esquivel Vazquez J and Goring S (2025) Package "clam": Classical Age-Depth Modelling of Cores from Deposits. Version 2.6.2. R Foundation for Statistical Computing. Available at: https://cran.r-project.org/web/packages/clam/index.html.

Bronk Ramsey C (2008) Deposition models for chronological records. *Quaternary Science Reviews* **27**(1), 42–60. doi: 10.1016/j.quascirev.2007.01.019.

Bronk Ramsey C (2009a) Bayesian analysis of radiocarbon dates. *Radiocarbon* **51**(1), 337–360. doi: 10.1017/S0033822200033865.

Bronk Ramsey C (2009b) Dealing with outliers and offsets in radiocarbon dating. *Radiocarbon* **51**(3), 1023–1045. doi: 10.1017/S0033822200034093.

Bronk Ramsey C (2023) Radiocarbon calibration: From bane to blessing. *Radiocarbon* 1–11. doi: 10.1017/RDC.2023.32.

Bronk Ramsey C (2024) OxCal, version 4.4. Available at: https://c14.arch.ox.ac.uk/oxcal.html.

Bronk Ramsey C, van der Plicht J and Weninger B (2001) "Wiggle matching" radiocarbon dates. *Radiocarbon* **43**(2A), 381–389. doi: 10.1017/S0033822200038248.

Cartereau M, Baumel A, Leriche A, Médail F, Santos Guerra A and Saatkamp A (2023) Germination niche of the endangered dragon tree *Dracaena draco* (L.) L. subsp. *draco* of the Macaronesian Islands. *Flora - Morphology, Distribution, Functional Ecology of Plants* **308**, 152405. doi: 10.1016/j.flora.2023.152405.

Durán I, Marrero Á, Msanda F, Harrouni C, Gruenstaeudl M, Patiño J, Caujapé-Castells J and García-Verdugo C (2020) Iconic, threatened, but largely unknown: Biogeography of the Macaronesian dragon trees (*Dracaena* spp.) as inferred from plastid DNA markers. *Taxon* **69**(2), 217–233. doi: 10.1002/tax.12215.

Giraldo JA, del Valle JI, González-Caro S, David DA, Taylor T, Tobón C and Sierra CA (2023) Tree growth periodicity in the ever-wet tropical forest of the Americas. *Journal of Ecology* **111**(4), 889–902. doi: 10.1111/1365-2745.14069.

Groenendijk P, Sass-Klaassen U, Bongers F and Zuidema PA (2014) Potential of tree-ring analysis in a wet tropical forest: A case study on 22 commercial tree species in Central Africa. *Forest Ecology and Management* **323**, 65–78. doi: 10.1016/j.foreco.2014.03.037.

Gupta D, Bleakley B and Gupta RK (2008) Dragon's blood: Botany, chemistry and therapeutic uses. *Journal of Ethnopharmacology* **115**(3), 361–380. doi: 10.1016/j.jep.2007.10.018.

Haines HA, Olley JM, English NB and Hua Q (2018) Anomalous ring identification in two Australian subtropical Araucariaceae species permits annual ring dating and growth-climate relationship development. *Dendrochronologia* **49**, 16–28. doi: 10.1016/j.dendro.2018.02.008.

Hall CM, James M and Baird T (2011) Forests and trees as charismatic mega-flora: Implications for heritage tourism and conservation. *Journal of Heritage Tourism* **6**(4), 309–323. doi: 10.1080/1743873X.2011.620116.

Hua Q, McDonald J, Redwood D, Drysdale R, Lee S, Fallon S and Hellstrom J (2012) Robust chronological reconstruction for young speleothems using radiocarbon. *Quaternary Geochronology* **14**, 67–80. doi: 10.1016/j.quageo.2012.04.017.

Hua Q, Turnbull JC, Santos GM, Rakowski AZ, Ancapichún S, De Pol-Holz R, Hammer S, Lehman SJ, Levin I, Miller JB, Palmer JG and Turney CSM (2022) Atmospheric radiocarbon for the period 1950–2019. *Radiocarbon* **64**(4), 723–745. doi: 10.1017/RDC.2021.95.

Jura-Morawiec J (2015) Formation of amphivasal vascular bundles in *Dracaena draco* stem in relation to rate of cambial activity. *Trees - Structure and Function* **29**(5), 1493–1499. doi: 10.1007/s00468-015-1230-3.

Jura-Morawiec J, Oskolski A and Simpson P (2021) Revisiting the anatomy of the monocot cambium, a novel meristem. *Planta* **254**(1), 6. doi: 10.1007/s00425-021-03654-9.

Krawczyszyn J and Krawczyszyn T (2014) Massive aerial roots affect growth and form of *Dracaena draco*. *Trees - Structure and Function* **28**(3), 757–768. doi: 10.1007/s00468-014-0987-0.

Lengálová K, Kalivodová H, Habrová H, Maděra P, Tesfamariam B and Šenfeldr M (2020) First age-estimation model for *Dracaena ombet* and *Dracaena draco* subsp. *caboverdeana*. *Forests* **11**(3), art. 264 (14 pp.). doi: 10.3390/f11030264.

Maděra P, Attorre F, Habrová H and Van Damme K (2021) Dragon trees, Tertiary relicts in current reality. *Forests* **12**(6), art. 756 (3 pp.). doi: 10.3390/f12060756.

Maděra P, Forrest A, Hanáček P, Vahalík P, Gebauer R, Plichta R, Jupa R, Van Rensburg JJ, Morris M, Nadezhdina N, Vaníčková L, Jura-Morawiec J, Wiland-Szymańska J, Kalivodová H, Lengálová K, Rejžek M and Habrová H (2020) What we know and what we do not know about dragon trees? *Forests* **11**(2), art. 236 (34 pp.). doi: 10.3390/f11020236.

Downloaded from https://www.cambridge.org/core. IP address: 217.74.153.144, on 01 Oct 2026 at 02:10:25, subject to the Cambridge Core terms of use, available at https://www.cambridge.org/core/terms. https://doi.org/10.1017/RDC.2025.10149

Marcinkiewicz J and Jura-Morawiec J (2024) New insight into secondary growth in roots of monocotyledons using the example of the dragon tree, *Dracaena draco* L. *Brazilian Journal of Botany* **47**(2), 399–404. doi: 10.1007/s40415-024-00997-x.

Palli J, Baliva M, Biondi F, Brienen R, Calcagnile L, D'Elia M, Quarta G, Siclari A and Piovesan G (submitted) Radiocarbon dating opens up new frontiers in the study of tree longevity.

Pearson S, Hua Q, Allen K and Bowman DMJS (2011) Validating putatively cross-dated *Callitris* tree-ring chronologies using bomb-pulse radiocarbon analysis. *Australian Journal of Botany* **59**(1), 7–17. doi: 10.1071/BT10164.

Piotrowska N, Vleeschouwer FD, Sikorski J, Pawlyta J, Fagel N, Roux GL and Pazdur A (2010) Intercomparison of radiocarbon bomb pulse and 210Pb age models. A study in a peat bog core from North Poland. *Nuclear Instruments and Methods in Physics Research Section B: Beam Interactions with Materials and Atoms* **268**(7), 1163–1166. doi: 10.1016/j.nimb.2009.10.124.

Reimer PJ, Austin WEN, Bard E, Bayliss A, Blackwell PG, Bronk Ramsey C, Butzin M, Cheng H, Edwards RL, Friedrich M, Grootes PM, Guilderson TP, Hajdas I, Heaton TJ, Hogg AG, Hughen KA, Kromer B, Manning SW, Muscheler R, Palmer JG, Pearson C, van der Plicht J, Reimer RW, Richards DA, Scott EM, Southon JR, Turney CSM, Wacker L, Adolphi F, Büntgen U, Capano M, Fahrni SM, Fogtmann-Schulz A, Friedrich R, Köhler P, Kudsk S, Miyake F, Olsen J, Reinig F, Sakamoto M, Sookdeo A and Talamo S (2020) The IntCal20 Northern Hemisphere radiocarbon age calibration curve (0–55 cal kBP). *Radiocarbon* **62**(4), 725–757. doi: 10.1017/RDC.2020.41.

Reimer PJ, Brown TA and Reimer RW (2004) Discussion: Reporting and calibration of post-bomb ^{14}C data. *Radiocarbon* **46**(3), 1299–1304. doi: 10.1017/S0033822200033154.

Reimer RW and Reimer PJ (2025) CALIBomb. Available at: http://calib.org/CALIBomb/.

Santos GM, Granato-Souza D, Ancapichún S, Oelkers R, Haines HA, De Pol-Holz R, Andreu-Hayles L, Hua Q and Barbosa AC (2024) A novel post-1950 CE atmospheric ^{14}C record for the tropics using absolutely dated tree rings in the equatorial Amazon. *Science of the Total Environment* **918**, 170686. doi: 10.1016/j.scitotenv.2024.170686.

Santos GM, Komatsu ASY, Renteria JM, Brandes AFN, Leong CA, Collado-Fabbri S and De Pol-Holz R (2023) A universal approach to alpha-cellulose extraction for radiocarbon analysis of ^{14}C-free to post-bomb ages. *Quaternary Geochronology* **74**, art. 101414 (15 pp.). doi: 10.1016/j.quageo.2022.101414.

Santos GM, Rodriguez DRO, Barreto NdO, Assis-Pereira G, Barbosa AC, Roig FA and Tomazello-Filho M (2021) Growth assessment of native tree species from the southwestern Brazilian Amazonia by post-ad 1950 ^{14}C analysis: Implications for tropical dendroclimatology studies and atmospheric ^{14}C reconstructions. *Forests* **12**(9), art. 1177 (18 pp.). doi: 10.3390/f12091177.

Santos GM, Southon JR, Griffin S, Beaupre SR and Druffel ERM (2007) Ultra small-mass AMS ^{14}C sample preparation and analyses at KCCAMS/UCI Facility. *Nuclear Instruments and Methods in Physics Research Section B: Beam Interactions with Materials and Atoms*, **259**(1), 293–302. doi: 10.1016/j.nimb.2007.01.172.

Santos GM and Xu X (2017) Bag of tricks: A set of techniques and other resources to help ^{14}C laboratory setup, sample processing, and beyond. *Radiocarbon* **59**(3), 785–801. doi: 10.1017/RDC.2016.43.

Silva L, Caujapé-Castells J, Lobo C, Casimiro P, Moura M, Elias RB, Fernandes F, Fontinha SS and Romeiras MM (2021) *Dracaena draco*, The IUCN Red List of Threatened Species 2021. International Union for Conservation of Nature and Natural Resources, e.T30394A119836316.

Soliz-Gamboa CC, Rozendaal DMA, Ceccantini G, Angyalossy V, van der Borg K and Zuidema PA (2011) Evaluating the annual nature of juvenile rings in Bolivian tropical rainforest trees. *Trees - Structure and Function* **25**(1), 17–27. doi: 10.1007/s00468-010-0468-z.

Stuiver M and Polach HA (1977) Discussion: Reporting of ^{14}C data. *Radiocarbon* **19**(3), 355–363. doi: 10.1017/S0033822200003672.

Tomlinson PB (2006) The uniqueness of palms. *Botanical Journal of the Linnean Society* **151**(1), 5–14. doi: 10.1111/j.1095-8339.2006.00520.x.

Tomlinson PB and Zimmermann MH (1969) Vascular anatomy of monocotyledons with secondary growth—an introduction. *Journal of the Arnold Arboretum* **50**(2), 159–179. doi: 10.5962/p.185758.

Wils THG, Robertson I, Eshetu Z, Sass-Klaassen UGW and Koprowski M (2009) Periodicity of growth rings in *Juniperus procera* from Ethiopia inferred from crossdating and radiocarbon dating. *Dendrochronologia* **27**(1), 45–58. doi: 10.1016/j.dendro.2008.08.002.

Xu X, Trumbore SE, Zheng S, Southon JR, McDuffee KE, Luttgen M and Liu JC (2007) Modifying a sealed tube zinc reduction method for preparation of AMS graphite targets: Reducing background and attaining high precision. *Nuclear Instruments and Methods in Physics Research Section B: Beam Interactions with Materials and Atoms* **259**(1), 320–329. doi: 10.1016/j.nimb.2007.01.175.

Cite this article: Biondi F, Santos GM, Palli J, Piovesan G, and Sosa PA (2026). Radiocarbon dating of a monumental dragon tree (*Dracaena draco* (L.) L.). *Radiocarbon* **68**, 1062–1070. https://doi.org/10.1017/RDC.2025.10149

Downloaded from https://www.cambridge.org/core. IP address: 217.74.153.144, on 01 Oct 2026 at 02:10:25, subject to the Cambridge Core terms of use, available at https://www.cambridge.org/core/terms. https://doi.org/10.1017/RDC.2025.10149